ELSEVIER

Surface Science 385 (1997) 66–76

surface science

Transmission electron microscopic investigation of an ordered Al_2O_3 film on NiAl(110)

M. Klimenkov [a], S. Nepijko [b], H. Kuhlenbeck [b], H.-J. Freund [a,b,*]

[a] *Lehrstuhl für Physikalische Chemie I, Ruhr-Universität Bochum, D-44780 Bochum, Germany*
[b] *Fritz-Haber-Institut der Max-Planck-Gesellschaft, Faradayweg 4–6, D-14195 Berlin, Germany*

Received 6 December 1996; accepted for publication 30 January 1997

Abstract

We have prepared under ultrahigh vacuum conditions a NiAl(110) wedge which was oxidized such that, after oxidation, small support-free Al_2O_3 crystallites were formed at the edge of the wedge, and the remaining part of the wedge was covered by a thin well-ordered Al_2O_3 film. This film, which has been characterized in great detail in earlier studies [J. Libuda et al., Surf. Sci. 318 (1994) 61], was transferred in air to a transmission electron microscope (TEM) and studied with respect to its geometric structure. The particular sample preparation allows for a direct comparison between the structure of the film and the bulk aluminum oxide. We find that the supported oxide exhibits a γ-Al_2O_3-like structure similar to that observed previously under UHV conditions, indicating that exposure to air has only a limited influence on the film. The lattice constant of the oxide film agrees within ~2% with that reported for bulk Al_2O_3. The domain structure of the alumina film as found in the ultrahigh vacuum experiments was also identified using TEM of the supported layer. The support-free oxide formed at the edge of the wedge exhibits the structure of the supported film formed under UHV conditions with deviations of the lattice constants of ~7% in one direction and ~1% in the other. © 1997 Elsevier Science B.V.

Keywords: Aluminum oxide; Electron microscopy; Epitaxy; Moiré-pattern

1. Introduction

In recent years several groups have used thin oxide films to prepare support materials for the study of model catalyst systems [1–5]. In order to fully exploit the potential of surface science tools these supporting films should be well structured. Typically, Al_2O_3 [1–5] and MgO [3–5] films have been prepared and used to support the deposition of small metal aggregates. The morphologies of the metal aggregates have been characterized in ultrahigh vacuum using scanning tunnelling microscopy (STM). In some cases, structural investigations with TEM have also been undertaken [3], but a systematic study in which a sample has been prepared in UHV and then transferred to the TEM via the atmosphere and analyzed with respect to the lattice parameters has, to the best of our knowledge, not been reported. We have studied Pt deposits on a thin Al_2O_3 film [6,7] and these results will be the topic of a forthcoming publication [8]. In the present study we report on results obtained on the pure support in order to investigate several specific questions:

* Corresponding author. Fritz-Haber-Institut der Max-Planck-Gesellschaft. Faradayweg 4–6, D-14195 Berlin, Germany. Tel.: +49-30-8413-4102, 4104; fax: +49-30-8413-4101; e-mail: freund@fhi-berlin.mpg.de

PII S0039-6028(97)00150-7

(1) Is it possible to determine the structure of the thin Al_2O_3 film (thickness ca. 5 Å) after transport of the sample through air?
(2) Does the structure of the thin film after transport through air correspond to that characterized under UHV conditions?
(3) As we go from supported alumina films to unsupported alumina how does the alumina structure change in comparison with a thin supported alumina film?

Answers to these questions are important in order to judge whether it will be possible, in the future, to transfer information derived from model systems based on thin film technology prepared under UHV conditions to more realistic conditions.

The supported alumina film was prepared via oxidation of a NiAl(110) alloy surface in UHV [9,10]. A very well-ordered Al_2O_3 film was formed with an average thickness of 4.5 Å. It was deduced on the basis of previous studies under UHV conditions that the material corresponds to γ-Al_2O_3 with [111] orientation, even though the thickness is not sufficient to contain a full γ-alumina unit cell perpendicular to the surface. The film grows in two domains on the NiAl(110) substrate. For samples prepared for use in TEM we find a γ-Al_2O_3-like structure for the thin supported film and the lattice of the unsupported oxide closely resembles that of the oxide layer formed under UHV conditions on NiAl(110). In both cases an accurate determination of lattice constants with reference to the NiAl substrate was possible.

2. Experimental

A bulk crystal disk of 3 mm diameter and 0.5 mm thickness was cut from a NiAl(110) rod along the (110) plane and oriented with an accuracy of about 1° by Laue diffraction. The disk was dimple-ground until the thickness in the middle of the disk was ≈80 μm. The disk was then milled in a fast ion etching system until a small hole of ≈0.2 mm diameter had been formed in the middle. The edge of the hole was wedge-shaped with a slowly varying thickness from 5 Å at the hole to ≈40 μm at the thicker parts of the disk. The area penetrable by electrons varied by about 70–150 nm from the edge of the hole into the sample at various locations. Such samples are suitable for TEM investigations [11].

The sample was transferred to an ultra-high-vacuum chamber with a working pressure of about 8×10^{-10} mbar. In the chamber it was attached to a sample holder formed from two thin tantalum foils of 0.0125 mm thickness, so that it was pinched between them allowing for preparation of both sides. The foils were spot-welded to a tantalum wire of 1 mm diameter. Heating was possible by passing an electric current through the foils. After cleaning the oxide by sputtering and annealing cycles it was prepared according to a procedure described elsewhere [9–11].

After oxide preparation and exposure to air the samples were transferred to an electron microscope "Hitachi-8100" with 200 keV acceleration voltage and 1.44 Å resolution. A double tilt specimen holder was used, which allowed for precise orientation of the specimen with respect to the electron beam.

An optical diffraction procedure with a laser wavelength of 632.8 nm was applied to analyze the TEM pictures. Some of the pictures were Fourier filtered.

3. Results and discussion

Fig. 1 gives a schematic representation of the oxidized wedge. In the region of the tip all substrate material is removed by sputtering and consequently support-free alumina crystallites are

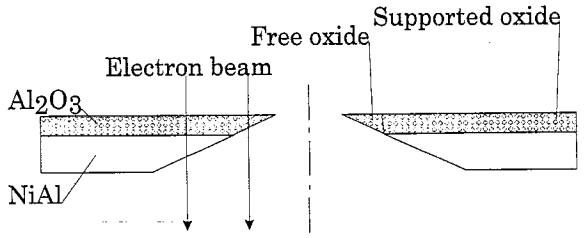

Fig. 1. Schematic representation of the wedge-shaped sample after oxidation.

Fig. 2. Transmission electron micrograph of Al_2O_3/NiAl(110); $E_{kin}=200$ keV, current density 1–10 Å cm^{-2}. Various areas with Moiré fringes are indicated with roman numbers.

formed. At the thicker parts, the wedge is covered with a thin oxide film.

Therefore, the present sample provides us with a thin film arrangement as well as with support-free Al_2O_3 crystallites 10–20 Å thick. TEM pictures were recorded for this sample, imaging simultaneously the thin film and the alumina crystallites. The structural parameters of the thin film and the crystallites may be compared directly. In the following we present and discuss the results for the thin film first and then report on the free oxide.

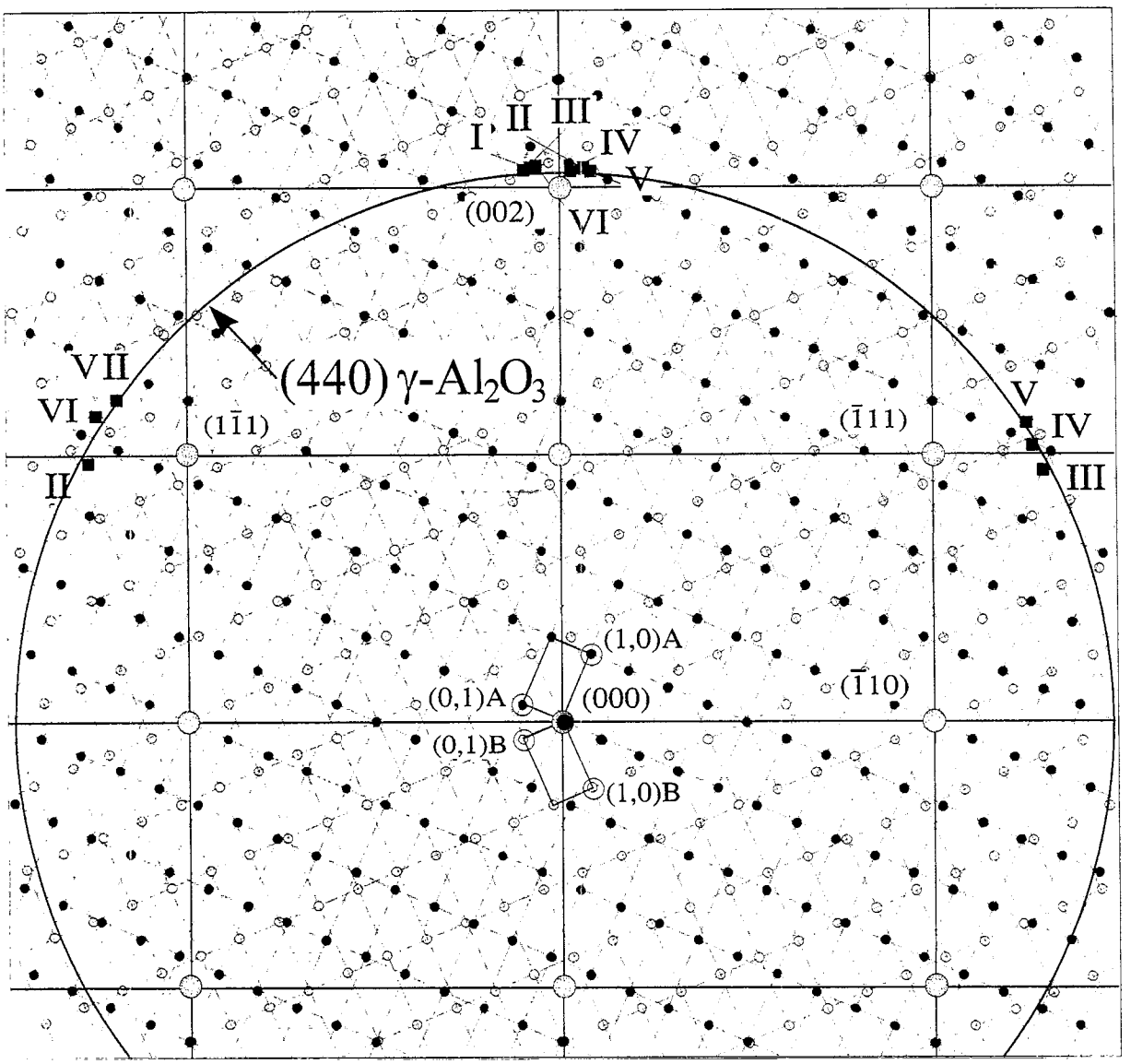

Fig. 3. Relative orientation of reciprocal spaces of NiAl(110) and the supported alumina film lattice as derived from LEED data [9,10]. The experimental points as determined from Fig. 2 are indicated by squares. Also shown is the intersection of the γ-Al_2O_3 (440) Ewald circle with the (110) plane.

3.1. Al_2O_3/NiAl(110)

Fig. 2a shows a TEM photograph of the thin Al_2O_3 film on the NiAl(110) surface. Two features are interesting for the present analysis. Firstly, the (001) crystallographic planes of NiAl with a separation of $d_{001}=2.873$ Å are visible over wide areas of the sample. This is an important observation because it provides us with a calibration for the length scale. Secondly, several sets of Moiré fringes [I–VII], due to double diffraction between the substrate and the alumina film, are observed [12–14]. Fig. 3 shows a diagram in reciprocal space of the relation between the NiAl(110) substrate

(shaded circles) and the reciprocal lattice of the oxide film formed under UHV conditions as obtained by LEED (open and black circles corresponding to two different domains of the oxide [9,10]).

Moiré patterns are due to electrons scattered by both the substrate and the oxide film. They are observed if the difference of the scattering vectors is small. If the scattering vector of the substrate and the k-vector of the Moiré pattern are known then the scattering vector of the oxide may be calculated. With $\boldsymbol{d}'_2$ being the scattering vector of the substrate, $\boldsymbol{d}'_1$ that of the oxide and $\boldsymbol{D}'$ the k-vector corresponding to the Moiré pattern, one obtains (see Fig. 4):

$$\boldsymbol{D}' = \boldsymbol{d}'_1 - \boldsymbol{d}'_2 \Rightarrow \boldsymbol{d}'_1 = \boldsymbol{D}' + \boldsymbol{d}'_2. \quad (1)$$

However, there is a general ambiguity in the determination of the oxide scattering vector since the direction of the k-vector of the Moiré pattern ($\boldsymbol{D}'$) is only known with an uncertainty of 180°. Therefore, two solutions for the problem exist and one has to find arguments which allow us to choose one of them.

From Fig. 3 it is obvious that there are several combinations of substrate and oxide lattice vectors of similar length and direction which are possible candidates for the formation of Moiré patterns. A prerequisite is that the scattering intensities for the combined scattering events are appreciable. Thus, it is favorable if the substrate reflection involved is rather intense. This is true under TEM conditions for the NiAl(002) and NiAl(111) reflections and consequently the combination vectors leading to Moiré fringes are grouped around these substrate reflections as shown in Fig. 3. The positions of the oxide scattering vectors as determined from the Moiré patterns in Fig. 2 using Eq. (1) are indicated in the figure by filled squares and roman numbers. The latter refer to the marked areas indicated in Fig. 2. As an example an enlargement of area III is shown in Fig. 5, where several Moiré fringes are superimposed. The NiAl substrate lattice constant is indicated at the top right. Two Moiré fringes are clearly observed and the periodicities are characterized by a_{M1} and a_{M2}. The directions of the corresponding k-vectors and the substrate reflections which gave rise to the Moiré fringes are indicated in the figure (for the notation, see Fig. 4). While a_{M1} is caused by scattering at a NiAl lattice vector in the [001] direction and an oxide film reflection, a_{M2} involves a substrate lattice vector in the NiAl[111] direction and another oxide reflection. The angles ω obtained from Fig. 5 are 112° and 189.5°, respectively. From the Moiré k-vector, the known substrate scattering vector and the measured angle ω, the deflection length

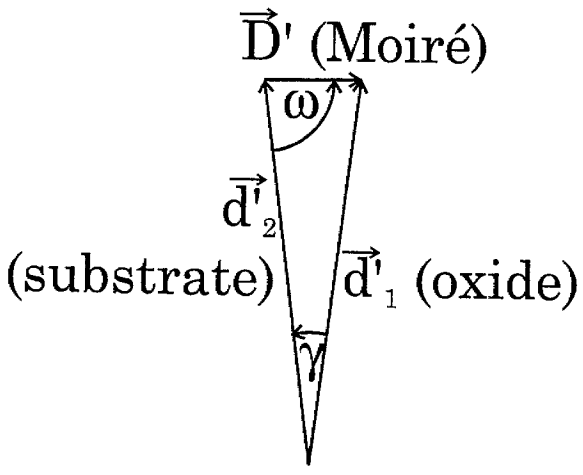

Fig. 4. Schematic drawing of the k-vectors involved in the formation of a Moiré pattern.

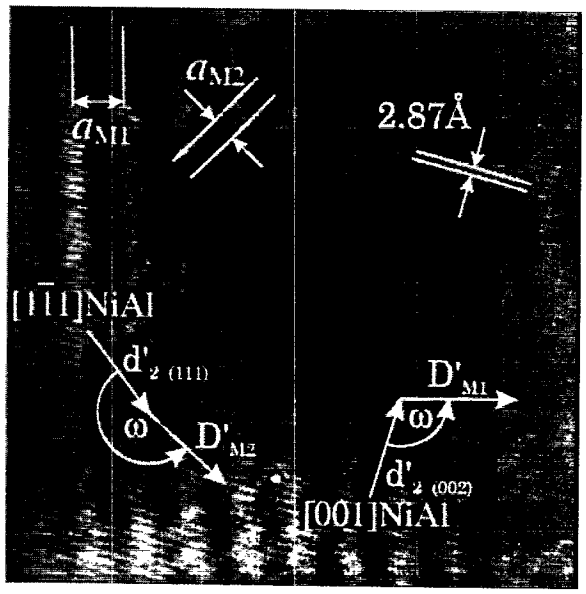

Fig. 5. Magnified view of area III of Fig. 2.

d_{reflex} was calculated in each case. The latter value is the inverse of the oxide scattering vector ($1/|\boldsymbol{d}'_1|$) and is calculated using the equation

$$d_{reflex} = \frac{1}{|\boldsymbol{d}'_1|} = \frac{1}{\sqrt{|\boldsymbol{d}'_2|^2 + |\boldsymbol{D}'|^2 - 2|\boldsymbol{d}'_2||\boldsymbol{D}'|\cos\omega}}. \quad (2)$$

This can be converted into an oxide lattice constant if a specific lattice is taken as reference. As noted above there are indications that the structure of the supported oxide film is similar to that of γ-Al_2O_3 [9,10]. Therefore, we chose the γ-Al_2O_3 lattice as a model for the unsupported oxide film. Its (440)-type lattice vector fulfils the Moiré scattering condition. The Ewald circle of the (440)-type lattice vector of γ-Al_2O_3 is indicated in Fig. 3 and the Moiré data points are grouped on this circle near the NiAl(002) and (111) reflections. Therefore, it is reasonable to relate the Moiré data derived from Fig. 2 to a γ-Al_2O_3-like structure. The ambiguity of the solutions of Eq. (1) was removed by considering only that solution for each set of data which yielded the best agreement between the calculated lattice constant and the literature value for γ-Al_2O_3. Table 1 contains the lattice constants as calculated from d_{reflex}. These values, which range from 7.83 and 7.93 Å, should be compared with 7.91 Å, i.e. the literature value for the lattice constant of γ-Al_2O_3 [15]. The deviations are of the order of 1 or 2%, thus the comparison appears to be justified. The fact that the structure of the oxide film as obtained using TEM resembles closely that of γ-Al_2O_3 may be viewed as an indication that the oxide layer is not considerably modified by the transport in air because the structure of the film as prepared in UHV also resembles that of γ-Al_2O_3.

As shown in Fig. 2, the areas of the sample exhibiting Moiré patterns are of the order of 150 Å by 300 Å wide. These areas are separated by both domain and antiphase domain boundaries, Fourier filtered examples of which are shown in Fig. 6a,b. Both defect structures have been identified for the film grown under UHV conditions on the basis of a LEED analysis and also an extended STM study [9,10]. The phase sensitivity of the Moiré pattern formation leads to considerable contrast at such defects. The arrows in Fig. 6a,b are used to highlight some of the domain boundaries. In the case of Fig. 6a the substrate structure is clearly visible as indicated by a_{100}. The domain boundary is directed along the substrate (110) direction.

The present analysis complements and corroborates an earlier study on considerably thicker oxide films with less pronounced lateral order on NiAl(110) reported by the Rühle group [16].

With the conclusion of the structural analysis of the supported oxide film using TEM we can now move on to consider the support-free alumina crystallites formed on the sample at the tip of the wedge.

3.2. *Support-free Al_2O_3*

Fig. 7a shows a larger area of the wedge near the edge where all NiAl has been oxidized and removed to form support-free Al_2O_3 crystallites. Fig. 7b is a close up of a typical area, chosen, however, deliberately near the NiAl substrate (darker region) in order to calibrate against the substrate structure, as indicated. The structural data of the unsupported oxide film deduced from an analysis of the pictures (such as Fig. 7a,b) are fully compatible with those from the supported alumina film. Clear crystallographic orientation is visible in various areas. The optical diffraction from one such area is shown in Fig. 8 (right) in direct comparison with a LEED pattern of the film (left). The comparison with the LEED pattern of the Al_2O_3/NiAl(110) system [9,10] recorded under UHV conditions (alluded to in Section 3.1) reveals remarkable correspondences. Of course, because the LEED data are an average over a very large area of the sample, and the TEM data stem from a local region, not all reflections representing different domains are reproduced. Numerical structural data derived from a detailed analysis of different areas indicated in Fig. 7a are listed in Table 2. The areas are denoted by the observed oxide lattice constants. The indexing refers to the grid of the LEED data of the alumina film as shown in Fig. 3. The lattice mesh of 9.84 Å × 18.1 Å is slightly different from the corresponding mesh derived from the LEED data, 10.6 Å × 17.9 Å. This difference may be traced back to the interaction of the supported oxide film

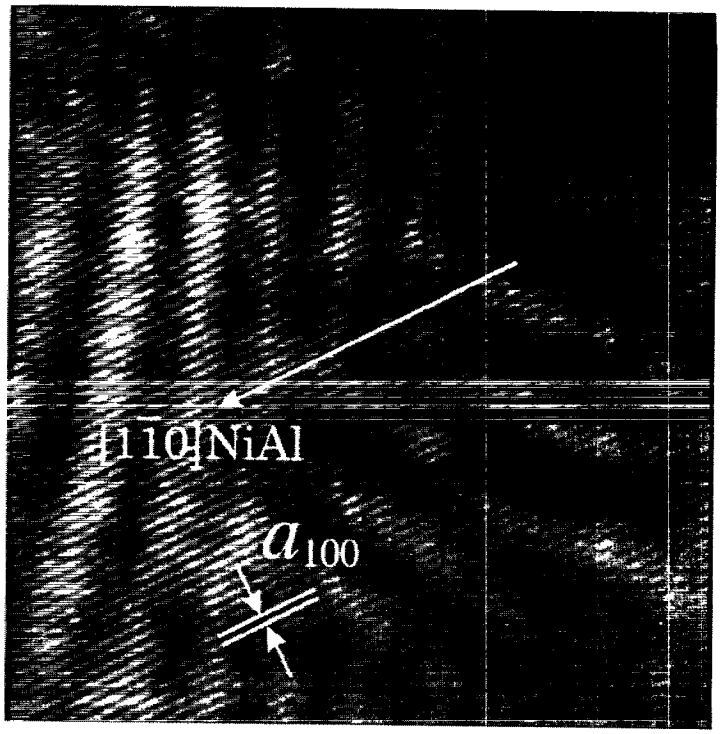

(a)

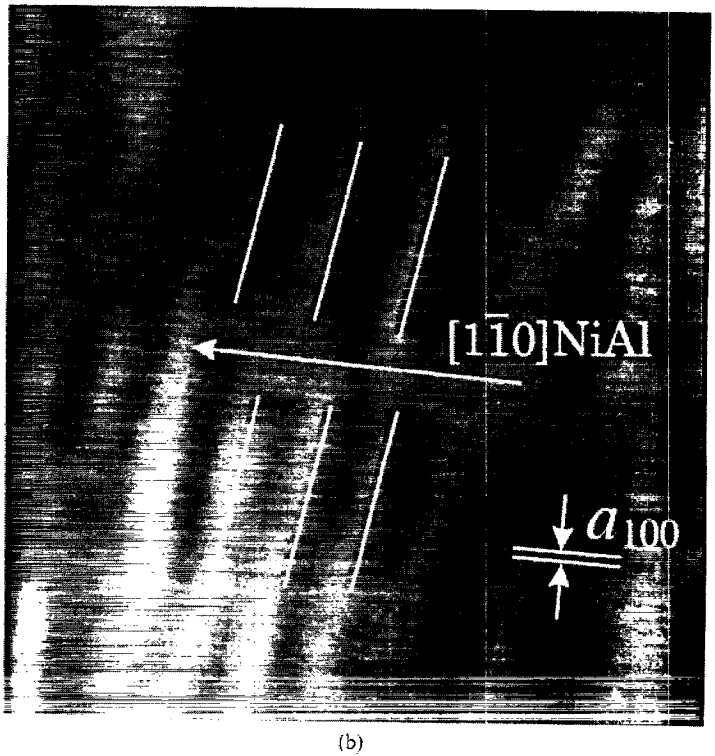

(b)

Fig. 6. Transmission electron micrographs of Al_2O_3/NiAl(110) showing domain (a) and antiphase domain (b) boundaries and other defects in the film.

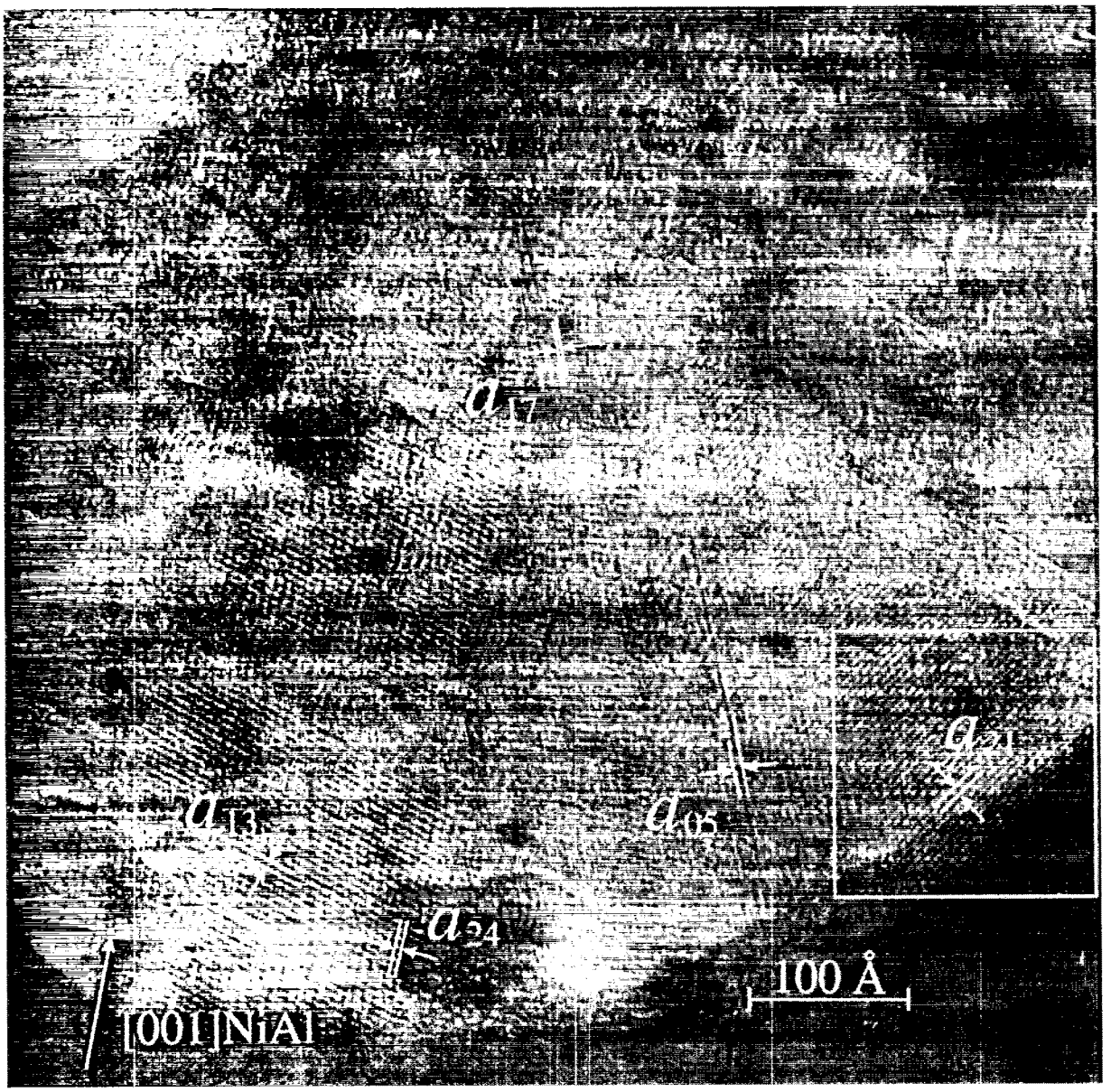

(a)

Fig. 7. (a) Transmission electron micrograph of the edge of the wedge where support-free Al_2O_3 formation takes place. The observed lattice parameters characteristic of the alumina film as determined by LEED (see Fig. 3) are indicated. (b) Magnified view of the area indicated in (a) near the border between the support-free alumina and the supported alumina film.

with the substrate giving rise to strain within the film, as has been pointed out previously [9,10]. This interaction is absent for the unsupported film.

In summary, we realize that the unsupported alumina resulting from oxidation of NiAl is very similar, but not identical, to the thin film and therefore most likely of γ-Al_2O_3-type. Since this means that the structure of the unsupported film is not, or at least not considerably, modified by transport through air we argue that this is also the

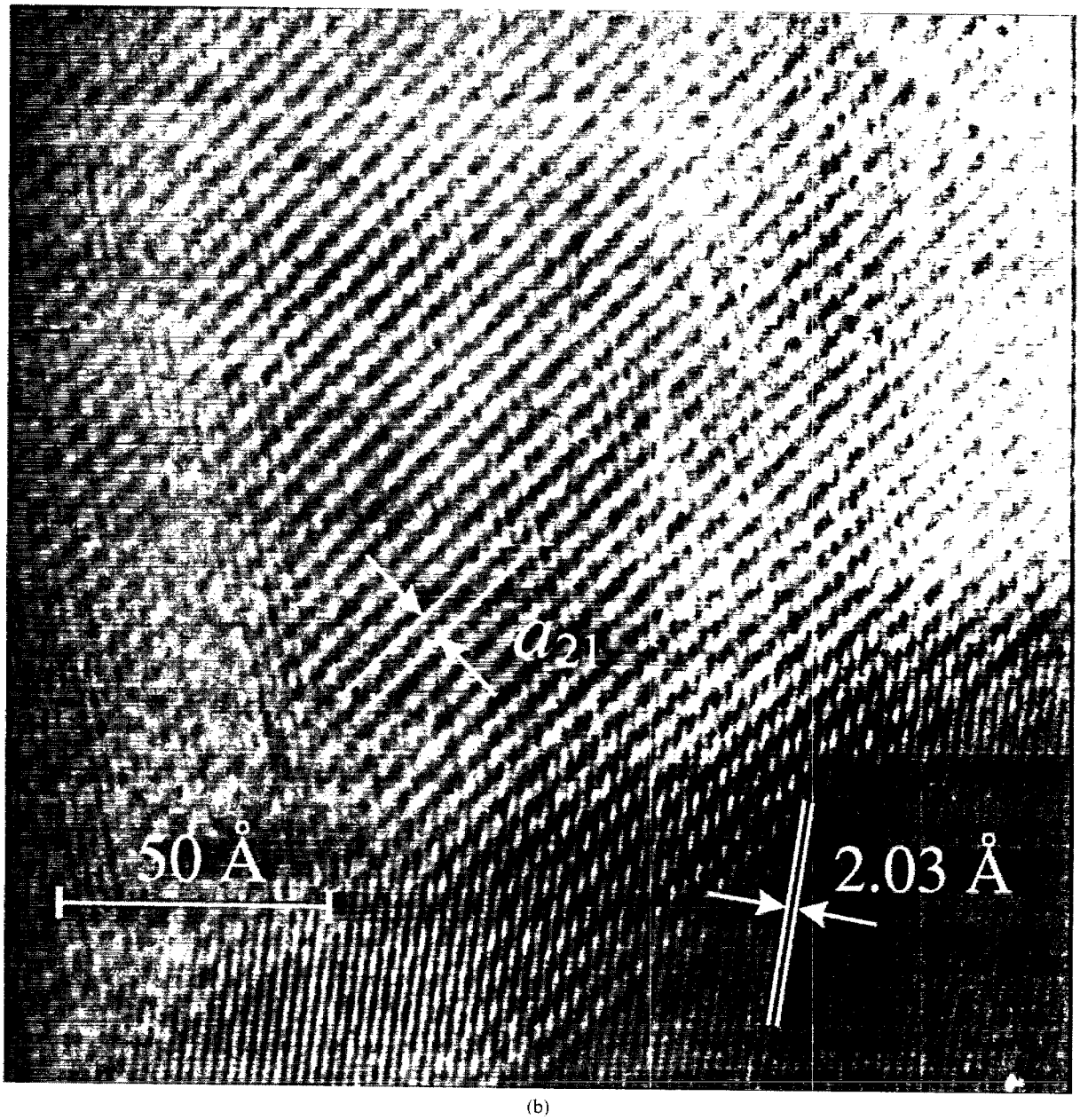

(b)

case for the supported film. The insensitivity of the unsupported oxide with respect to exposure to air is a very important finding with respect to the deposition of metal aggregates, which we shall report in a subsequent publication [8].

4. Synopsis

We have demonstrated that structural data gained by TEM on a thin alumina film grown on a NiAl(110) substrate after exposure to air are

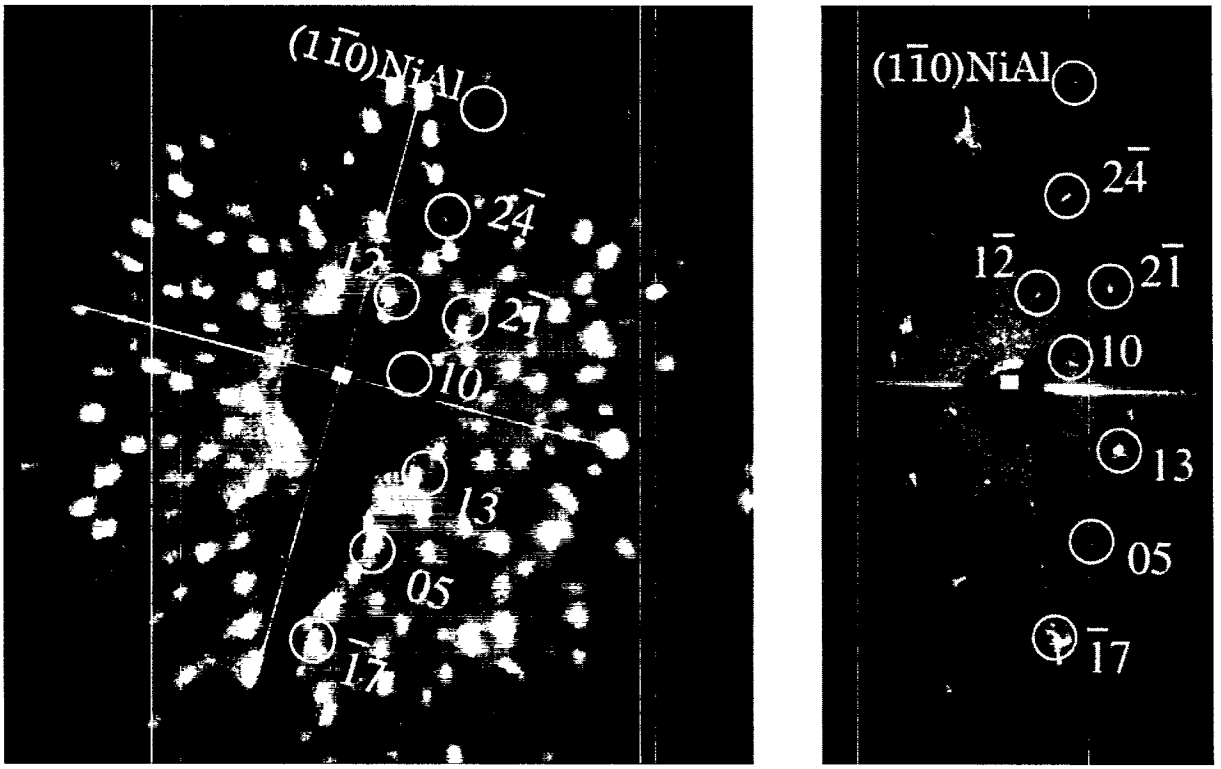

Fig. 8. Optical analysis (right) of the TEM picture (Fig. 7a) in comparison with the LEED pattern observed under UHV conditions.

Table 1
Quantitative information deduced from the analysis of Fig. 2. The roman numbers refer to the areas indicated in Fig. 2. According to literature data the lattice constant of γ-Al_2O_3 is 7.91 Å [15]

Area	NiAl scattering vector	Moiré periodicity (Å)	ω	d_{reflex} (Å)	Calculated oxide lattice constant (Å)
I	[002]	23.7	117°	1.396	7.90
II	[002]	24.5	241°	1.395	7.89
III	[002]	18.2	112°	1.392	7.87
IV	[002]	39.3	206°	1.391	7.87
V	[002]	21.8	238.5°	1.387	7.85
VI	[002]	21.2	122.5°	1.384	7.83
II	[$\bar{1}$11]	8.80	169.5°	1.399	7.91
III	[1$\bar{1}$1]	8.90	189.5°	1.401	7.92
IV	[1$\bar{1}$1]	7.58	215°	1.400	7.92
V	[$\bar{1}$11]	8.19	161.5°	1.389	7.86
VI	[1$\bar{1}$1]	7.89	210°	1.398	7.91
VII	[1$\bar{1}$1]	8.55	181°	1.389	7.86

comparable to data recorded for the same system under UHV conditions. The TEM data support the idea that the Al_2O_3/NiAl(110) film exhibits a structure which is similar to that of γ-Al_2O_3. The sample preparation allows for a parallel investigation of the thin film and a support-free bulk alumina sample.

We believe that the present study gives us confi-

Table 2
Quantitative information deduced from an analysis of Fig. 7a. The indexing refers to the reciprocal lattice of the thin alumina film as prepared in UHV (Fig. 3)

No.	Index	LEED (Å)	Optical diffraction (Å)
1	$A(1,3)$	5.23	5.15
2	$A(2,\bar{1})$	5.08	4.66
3	$A(\bar{1},7)$	2.49	2.45
4	$A(2,\bar{4})$	3.44	3.34
5	$A(1,\bar{2})$	6.89	6.68
6	$A(1,0)$	10.6	9.84
7	$A(0,5)$	3.57	3.61

dence to use TEM data in an attempt to understand model catalyst systems based on thin film preparation.

Acknowledgements

We could not have carried out the present work without support from the Deutsche Forschungsgemeinschaft (Forschergruppe "Modellkat") and the Ministerium für Wissenschaft und Forschung des Landes Nordrhein-Westfalen through Referat IV A5 (D. Dzwonnek). We are grateful to Dr. K. Weiss from the Fritz-Haber-Institut der Max-Planck-Gesellschaft for help with the optical diffraction analysis.

References

[1] H.-J. Freund, Angew. Chem. 36 (1997) 452.
[2] M. Bäumer, J. Libuda, H.-J. Freund, NATO Adv. Study Institute, Erice, Italy, Kluwer, Dordrecht, 1997.
[3] S.K. Purnell, X. Xu, D.W. Goodman, B.C. Gates, Langmuir 10 (1994) 3057; J Phys. Chem. 98 (1994) 4076.
[4] M.C. Wu, W.S. Oh, D.W. Goodman, Surf. Sci. 330 (1995) 61.
[5] D.W. Goodman, Chem. Rev. 95 (1995) 523; Surf. Rev. Lett. 2 (1985) 9.
[6] F. Winkelmann, G. Wohlrab, J. Libuda, M. Bäumer, D. Cappus, M. Menges, K. Al-Shamery, H. Kuhlenbeck, H.-J. Freund, Surf. Sci. 307-309 (1994) 1148.
[7] Th. Bertrams, F. Winkelmann, Th. Uttich, H.-J. Freund, H. Neddermeyer, Surf. Sci. 331-333 (1995) 1515.
[8] M. Klimenkov, S. Nepijko, H. Kuhlenbeck, M. Bäumer, R. Schlögl, H.-J. Freund (to be published).
[9] R.M. Jaeger, H. Kuhlenbeck, H.-J. Freund, M. Wuttig, W. Hoffmann, R. Franchy, H. Ibach, Surf. Sci. 259 (1991) 235.
[10] J. Libuda, F. Winkelmann, M. Bäumer, H.-J. Freund, Th. Bertrams, H. Neddermeyer, K. Müller, Surf. Sci. 318 (1994) 61.
[11] M. Klimenkov, PhD Thesis, Ruhr-Universität-Bochum, 1997 (to be published).
[12] P.B. Hirsch, A. Howie, R.B. Nicholson, D.W. Pashley, M.J. Whelan, Electron Microscopy of Thin Crystals, Butterworth, London, 1965.
[13] T. Isshiki, M. Ohta, K. Nishio, M. Shiojiri, Thin Solid Films 271 (1995) 84.
[14] S.A. Nepijko, E. Pippel, J. Woltersdorf, Phys. Status Solidi (a) 61 (1980) 469.
[15] R.W.G. Wyckoff, Crystal Structures, 2nd ed., Wiley-Interscience, New York, 1965.
[16] J.C. Yang, E. Schumann, M. Müllejans, M. Rühle, Phys. D: Appl. Phys. 29 (1996) 1718.